

# ‘Application of camera based methods for study of oxygen enriched premixed ethylene/air flames

Y. Ögren<sup>\*1,2</sup>, A. Sepman<sup>1</sup>, H. Wiinikka<sup>1,2</sup>

<sup>1</sup>SP-Energy Technology Center AB, Box 726 SE-941 28, Piteå

<sup>2</sup>Luleå University of Technology, Energy Engineering, Division of Energy Science, SE-971 87, Luleå, Sweden

## Abstract

The measurements of soot absorption and flame temperature were performed in flat fuel-rich C<sub>2</sub>H<sub>4</sub>-O<sub>2</sub>-N<sub>2</sub> flames with O<sub>2</sub> Concentrations from 21-50% using a two color pyrometer and a direct laser absorption system. The soot concentration measured by the two methods are generally in a good agreement. The soot concentration increases with the increase in O<sub>2</sub> and equivalence ratio. The maximum temperature did not increase significant with oxygen addition or changes in equivalence ratio.

## Introduction

To produce CO<sub>2</sub> neutral bio based motor fuels gasification of biomass is one possible solution. At SP Energy Technology Center (SP ETC) in Piteå entrained flow gasification of biomass is in focus of research on gasification/ renewable motor fuel processes. It has been shown in earlier work that monitoring the gasification process can be done effectively with a simple camera installed in N<sub>2</sub> flushed probe[1-3]. The camera helps the operator to see the most obvious process failures that can happen inside a gasifier (e.g. flame instabilities and plugging of the slag tapping hole). Efficient optimization of the system often requires more sophisticated experimental methods capable providing the fast qualitative or, preferably, quantitative information on an important parameters of the process, such as temperature and soot concentration inside the hot reactor. The temperature is a key gasification parameter responsible for the efficiency of the process. During a woody-biomass gasification a considerable amount of soot is produced [2, 4], which may significantly influence the thermal efficiency [5] and causes deposition and pollution. Two color pyrometry is well established method [6,7] capable of fast simultaneous detection of both the temperature and soot concentration in flames. Here we report the progress in the development of the two color sensor for the optimization of a gasification process based on the color pyrometry technique. Since the immediate application of the method to such complex environment as a gasifier is hard, we choose to first apply the sensor to well-defined flat flames. To check the performance of the developed pyrometer over the wide range of flame parameters, we performed measurements of the temperature and soot concentration in fuel-rich flat ethylene-O<sub>2</sub>-N<sub>2</sub> flames at different equivalence ratios. The O<sub>2</sub>/N<sub>2</sub> ratio was also varied to bring the conditions studied closer to those occurring in a real gasification process. The two color pyrometer measurements regarding soot are compared with direct laser absorption technique and for temperature with the predictions of detailed flame calculations.

## Background of pyrometry

Pyrometry is a method based on Planck’s law of radiation

$$I_b(T, \lambda) = \frac{2hc^2}{\lambda^5} \frac{1}{e^{\frac{hc}{\lambda T k_b}} - 1} = \frac{c_1}{\lambda^5} \frac{1}{e^{\frac{c_2}{\lambda T}} - 1} \quad (1)$$

Where  $I_b$  is the emitted radiation from a black body as a function of temperature  $T$  and wavelength  $\lambda$ ,  $c$  is the speed of light,  $h$  is Planck’s constant and  $k_b$  is the Stefan Boltzmann constant. Using Eq. (1) it is possible to determine the temperature of a black body by comparing the radiation from two wavelengths. The emissivity of soot can be written as.

$$I_g = \epsilon(T, \lambda) I_b \quad (2)$$

Using Wien’s approximations of Planck’s law valid for optical part of the spectra the following equation can be obtained [8]

$$T = \frac{c_2 \left( \frac{1}{\lambda_2} - \frac{1}{\lambda_1} \right)}{\ln \left( \frac{I_1}{I_2} \right) + \ln \left( \frac{\epsilon_{\lambda_2}}{\epsilon_{\lambda_1}} \right) + 5 \ln \left( \frac{\lambda_1}{\lambda_2} \right)} \quad (3)$$

Where  $I_1$  and  $I_2$  are the intensity of light collected at  $\lambda_1$  and  $\lambda_2$ , respectively. For applying Eq. (3) a calibration is using a well-defined radiation source is assumed, this to validate the ratio measured by the system.

To solve this equation an assumption about emissivity is needed. For sooty flames, two approaches are generally used. In the first one, the emissivity of soot is assumed to be independent of wavelength, in this case the ratio for the two emissivities is one.

In the second approach following the research of Hottel et al [9], the emissivity is expressed as

\* Corresponding author: [yngve.ogren@etcpitea.se](mailto:yngve.ogren@etcpitea.se)

$$\epsilon_\lambda = 1 - T_\lambda = 1 - e^{-\frac{kL}{\lambda^\alpha}} \quad (4a)$$

Where  $T_\lambda$  the transmission of the signal,  $k$  is the wavelength independent adsorption coefficient,  $L$  the path length  $\alpha$  is an empirical coefficient where 1.39 is used [6, 9]. When this equation is combined with the general description of emissivity Eq. (2) and Planck's law Eq. (1), one can get the following equation

$$kL = -\lambda^\alpha \ln \left( 1 - \frac{\frac{c_2}{e^{\lambda T}} - 1}{\frac{c_2}{e^{\lambda T_a}} - 1} \right) \quad (5)$$

Where  $T_a$ , is the apparent temperature of the object, by equating the right sides of Eq. (5) for two different wavelengths the true temperature can be determined with

$$\left( 1 - \frac{\frac{c_2}{e^{\lambda_1 T}} - 1}{\frac{c_2}{e^{\lambda_1 T_{a1}}} - 1} \right)^{\lambda_1^\alpha} = \left( 1 - \frac{\frac{c_2}{e^{\lambda_2 T}} - 1}{\frac{c_2}{e^{\lambda_2 T_{a2}}} - 1} \right)^{\lambda_2^\alpha} \quad (6)$$

Calibration of temperature-light intensity is required to get  $T_{a1}$  and  $T_{a2}$  temperatures and solve Eq. (6). A blackbody radiator or a tungsten lamp is typically used for this purpose. The  $kL$  factor can be directly related to the soot volume factor according to [8] describing emissivity dependence of soot as

$$\epsilon_\lambda = 1 - e^{-\frac{P_1 f_v}{\lambda^\alpha}} \quad (4b)$$

Where  $f_v$  is the soot volume fraction,  $P_1$  is a parameter in the range 4.9-6 [8]. Since  $k$  is directly proportional to  $f_v$ , the comparison of the soot formation in different flames can be performed by analyzing the absorption coefficient. The comparison between the pyrometer and the laser absorption was done by translating the  $kL$  to wavelength dependent  $KL$  with

$$KL_{\lambda_1} = kl \left( \frac{\lambda_1}{\lambda_2} \right)^\alpha \quad (7)$$

Where the used and desired wavelength is inserted.

Temperature in the flames was determined by two approaches. The first, Eq. (3), where wavelength independence of soot emissivity is assumed, (the ratio method). The second follows the method, developed in [9] using Eq.(6).

The first pyrometers consisted of a pipe with a tungsten filament which the hot object was compared with, when they glow equally much they have the same apparent temperature [9]. Today the usual approach is to get a camera with a CCD or CMOS sensor. Common applications for pyrometers are measuring temperature and soot/absorption in diesel combustion [7] and coal flames [6].

### Burner system

A water cooled sintered stainless steel McKenna burner was used to generate well-defined flat flames. The

burner is 60mm in diameter and has the 5 mm thick outer ring which can be used for nitrogen co-flow. The McKenna burner used in the experiments has a center tube. The center tube allows additives to the flame which is planned for future research. The burner was placed in a 250 mm square co-flow box where flows up to 1000 L/min of nitrogen can be obtained. The nitrogen shields the flame from ambient air. The equivalence ratio was controlled using calibrated mass flow controllers (Bronkhorst). The maximum uncertainty in the equivalence ratio due flow controller error was estimated to be  $\pm 1.55\%$ . To improve stability of flames a 60 mm circular plate of thick stainless steel was placed approximately 21 mm above the burner similarly to [10] and [11]. The setup is schematically shown in Figure 1

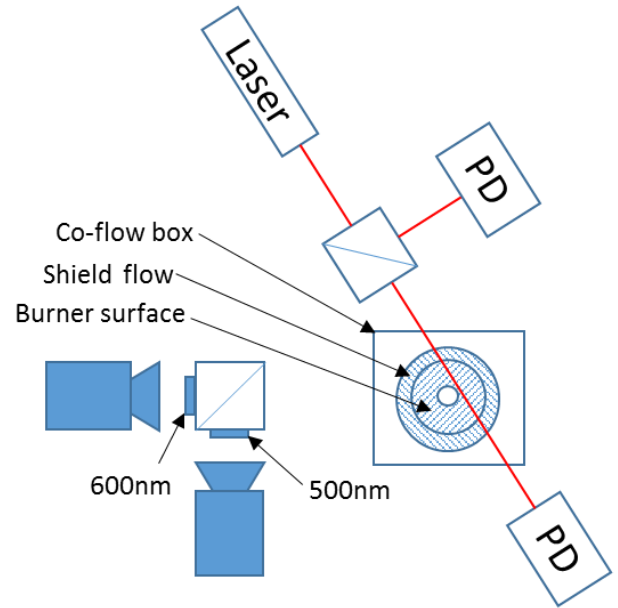


Figure 1. Experimental setup

The burner was operated with ethylene premixed with artificial air with different N<sub>2</sub>/O<sub>2</sub> ratio. A fixed total volume flow of 10 L/min was used for all flames. The nitrogen shield gas was set to 5L/min and the box co-flow of nitrogen was 800L/min giving an oxygen free environment round the flame. To measure soot absorption profile with the laser, the burner was transported along Z-axis with a lab-jack (Thorlabs). The flames investigated are reported in table 1.

Table 1. Experimental settings and calculated temperatures

Case	$\phi$	O <sub>2</sub> [%]	Adiabatic Temperature [K]	Wang [K]
A1	2.0	21	1906	1685
A2	2.0	25	2086	1711
A3	2.0	30	2275	1737
A4	2.5	25	1795	1656
A5	2.5	35	2081	1697
A6	2.5	45	2279	1723
A7	3.0	30	1656	1609
A8	3.0	40	1844	1637
A9	3.0	50	1984	1656

For each flame studied the table also includes the adiabatic temperature and the maximal calculated temperature with PREMIX code from the CHEMKIN II package [12] using reaction scheme developed by Qin et al [13]. This mechanism includes hydrocarbons up to two benzene rings.

#### Pyrometer and laser absorption set ups

A two color pyrometer was built with two monochromic CCD cameras (Basler acA780-75 gm) which were used in an 8bit sampling mode triggered electrical with a signalgenerator (TTi TG330) used with 30Hz square waves for simultaneous sampling. Two Fujifilm HF50HA-1 lenses with 50mm focal length and F-number sat to 4 was mounted on the cameras. For sorting the pictures in two wavelengths 600 and 500nm bandpassfilters 10 nm wide were used, together with a dichroic beam splitter (Thorlabs DMLP567R). Schematic of the system can be seen in Figure 1. The data was collected with a PC using MATLAB.

The system was calibrated with a Dias black body furnace between 900°C and 1500 °C in increments of 50 °C. Linearity and homogeneous of the system was also investigated with the blackbody radiator. The dark noise from the camera was however estimated to be between 0-1 grey values when using the camera in 8-bit mode. Another source of error is the ambient light in the room which can interfere with this system. This contribution to the signal is however very small compared to the flame and is also estimated to be around 0-1 grey value.

The measured data was treated with Eq. (6) for temperature and Eq. (5) for KL where 600nm is used as wavelength.

In the laser absorption measurements, the collimated beam from the diode laser (S2011, Thorlabs), at 635 nm, was directed through the flame. Before entering the flame, part of the laser beam was split off to produce the reference signal. The powers of the reference and sample beams were measured by New Focus 2031 large-area photodiodes with internal amplifiers. The photodiode signals were sampled by the digital oscilloscope (ME-UM202, Melihaus) and processed by a PC. The background signals were measured with the laser blocked. The measured data from the photodetectors

where translated to the pyrometers wavelength 600nm with E.q (7) from 635nm.

#### Results and Discussion

To illustrate the performed measurements, we present two-dimensional false color plots of the temperature (Figure 2) and soot absorption (Figure .3) for case A5. The beginning of the vertical scale, 0 mm, matches the position of the burner surface. Furthermore, the plate is located at 21 mm distance. The calculations are made using Eq. (6).

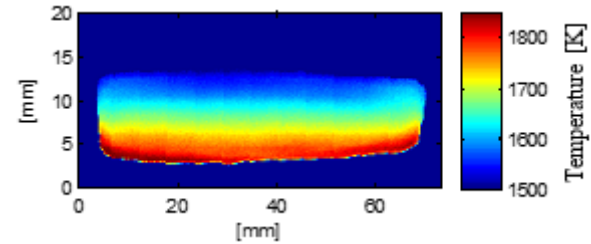


Figure 2. Temperature of A5 calculated with Eq. (6)

One dimensional character of the flame is clearly seen from Figure 2. Since the temperature changes only in the vertical direction. The flame maximum temperature is approximate 1800 K at a distance 4-5 mm above the burner surface and then decrease thereafter slowly over the measured height. The decrease is caused by the flame radiation. The maximal temperature of this burner stabilized flame is well below the corresponding adiabatic temperature, the difference is almost 300 K and is in reasonably good agreement with the maximal temperature calculated using Qin et al. [13] chemical mechanism for this flame, see Table 1.

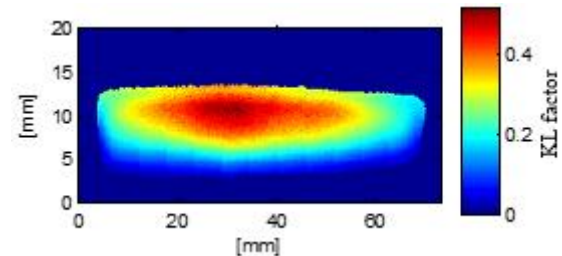


Figure 3. Soot absorption for flame A5

The absorption factor, (Figure 3) increases generally with the height and displays also radial variation expected due to the difference in the absorption path length while going from the center of the burner to its edges.

For convenience of the comparison of the temperatures and absorption factors measured by different techniques in different flames, below we restrict the representation of the experimental results to the vertical profiles. Figure 4 shows the temperature T and soot absorption KL factor measured in flames with the equivalence ratio 2 (cases A1, A2 and A3) as a function of the distance from the burner surface. Since all studied here flames were strongly stabilized, the soot captured using our present pyrometer set up (starting above 4 mm) occurs above the main reaction zone of the flames. Generally no large difference in the temperature profiles

is noticed for the different flames. The flame temperatures for 25 and 30% of  $O_2$  in the synthetic air (cases A2 and A3) display the same behavior decreasing from 1800 K to 1690 K over the span of 8 mm (from 5 to 13 mm height). The maximal flame temperature for A1 case is about 1900 K, the temperature decreases as a function of the height, reducing to the value of 1700 K at 13 mm height. We note that the 1-D flame calculations for cases A1-A3 show that the maximal temperatures reached within first 2-3 mm from the burner are within 50 K from each other.

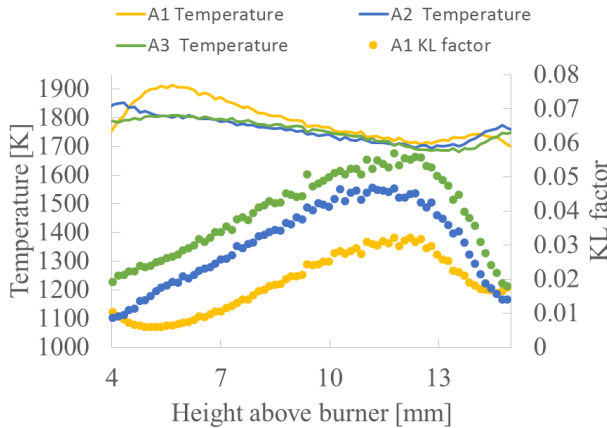


Figure 4. Soot and Temperature for flame A1-A3 with respect to height.

All three temperature profiles show an small upturn above 13 mm. Turning to the soot profiles, we note that they increase with the height for all flame studied up to approximately 12-13 mm distance, then decrease rapidly. Furthermore, the soot amount increases with the increased amount of oxygen added to the air. This observation is also valid for the flames at other studied equivalence ratio. We believe that the behavior of the  $T$  and  $KL$  profiles above 12 mm height is strongly influenced by the uncertainties of our measurements, see below.

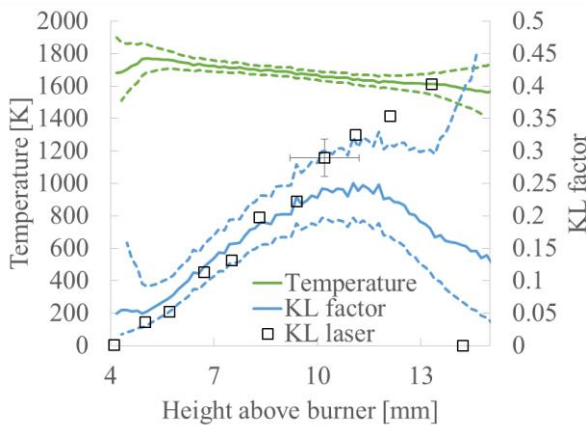


Figure 5. Comparison between the Pyrometer and laser absorption for flame A4.

Figure 5 displays the absorption factor measured using the two color pyrometer and direct absorption technique in Case A5 as a function of the distance from the burner surface. The figure also includes the measured temperature and uncertainties curves for  $T$  and  $KL$  profiles due to the detection limit of our cameras. The uncertainty are estimated by calculating  $T$  and  $KL$  with intensities from two cameras displaced with two gray values. To avoid showing the data points with very large uncertainties we chose to include in the figures the data for which the corresponding intensities are above 3 gray scale values. Comparison of the soot absorption profiles measured by two techniques demonstrate the very good agreement up to approximately 10 mm height; the profiles grow linearly reaching the value 0.25 at this distance. The profile measured by the direct laser absorption measurements continues its growth above the distance, while the data obtained using two color pyrometer do not change significantly at the next few mm and then decline. The temperature profile demonstrates the modest decrease with the height, with the rate similar to that for A1-A3 flames. The uncertainties reported in the figure suggest that the accuracy of the temperature and absorption data are strongly deteriorated above 10 mm. Considering above and since the soot consumption requires an oxidizer, which was not present in our system due to protective  $N_2$  flow around the burner at this distance, we believe that the divergence of the  $KL$  profiles is the result of the uncertainties in our two-color method. We plan to investigate the accuracy of our measurements in more details in future.

Figure 6 shows the flame temperatures evaluated via Eq. (3) assuming that the emissivity is independent on the wavelength (ratio) and via Eq. (6). It is seen as

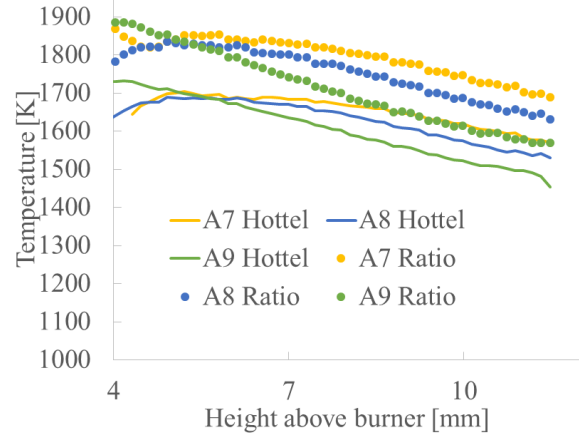


Figure 6. Temperatures for flame A7-A9, where temperatures have been calculated using both presented methods.

expected that the ratio method gives the higher temperature (between 125 and 175 K) then one assuming the wavelength dependence of soot emissivity. Apart from this temperature shift, there is no significant difference between the profiles evaluated by two methods for all cases shown. The 1-D flame calculations support the Hottel's method of the evaluation of temperature.

## Conclusions

Two color pyrometer is used to study the effects of varying equivalence ratio and O<sub>2</sub> concentration in the synthetic air on soot and temperature in fuel-rich ethylene-O<sub>2</sub>-N<sub>2</sub> flames. The soot concentration increases almost linearly for all studied flames at least up to the distance of 10 mm from the burner surface. The further efforts required to validate the experimental data at higher distances. We measured an increase in soot absorption with the increase of oxygen in the syntactic air at a given equivalence ratio, it also increases with the increase of equivalence ratio. The comparison of the vertical absorption profiles measured using the two color pyrometer and direct absorption techniques demonstrate a good agreement up to the distance of 10 mm. The temperature vertical profiles decline gradually with the height in the measurement domain between 4 and 12 mm, with the rate similar for all flames studied. The maximal flame temperatures evaluated assuming the wavelength dependent soot emissivity formulated by Hottel agree within about 100 K and usually better with those obtained from calculations using Qin et. al mechanism.

## Acknowledgment

This work has been performed within the platform for entrained flow gasification (Bio4Gasification) in the Swedish Centre for Gasification financed by the Swedish Energy Agency and the member companies.

## References

- [1] F. Weiland, H. Hedman, M. Marklund, H. Wiinikka, O. Öhrman, R. Gebart. 2013, *Energ Fuel* 27 (2013) 932-941.
- [2] F. Weiland, P. Nilsson, H. Wiinikka, A. Gudmundsson, R. Gebart, M. Sanati. 2014, *Aerosol Sci. Technol.* 48 (2014) 1145-1155.
- [3] P. Carlsson, C. Ma, R. Molinder, F. Weiland, H. Wiinikka, M. Öhman, O. Öhrman. 2014, *Energ Fuel* 28 (2014) 6941-6952.
- [4] H. Wiinikka, F. Weiland, E. Pettersson, O. Öhrman, P. Carlsson, J. Stjernberg. *Combust. Flame* 161 (2014) 1923-1934.
- [5] F. Weiland, H. Wiinikka, H. Hedman, J. Wennebro, E. Pettersson, R. Gebart. To be submitted to *Fuels*.
- [6] G. Lu, Y. Yan. *IEEE T Instrum Meas* 55 (2006) 4.
- [7] M. Jakob, P. Lehnen, P. Adomeit, S. Pischinger. *Combust. flame* 161 (2014) 2825-2841.
- [8] N. Docquier, S. Candel. 202, *Prog Energ. Combust.* 28 107-150.
- [9] H. Hottel, F.P. Broughton, *Indust. Eng. Chem. Anal. Ed.* 4 (2) (1932) 166-175.
- [10] H. Bladh, J. Johnsson, N-E. Olofsson, A. Bohlin, P-E. Bengtsson. 2011, *P Combust Inst.* (2011) 33 641-648.
- [11] R. Hedef, K.P Geigle, W. Meier, M. Aigner. , *Int. J. Therm. Sci* 49 (2010) 1457-1467.
- [12] R. Kee, F. Rupley, J. Miller (1989) Report N 89-8009.
- [13] ZW. Qin, VV. Lissianski, HX. Yang, WC Gardiner, SG. Davis, H. Wang. *P Combust Inst* 28 (2000) 1663-1669.
- [14] J. Warnatz, U. Maas, R.W Dibble. *Combustion Springer (2006)*. s.l.